Friction **11**(3): 410–424 (2023)
https://doi.org/10.1007/s40544-022-0605-x
ISSN 2223-7690
CN 10-1237/TH
RESEARCH ARTICLE

Dopamine-triggered one-step functionalization of hollow silica nanospheres for simultaneous lubrication and drug release

Qiangbing WEI[1,*], Tian FU[1,2], Lele LEI[1], Huan LIU[1,2], Yixin ZHANG[1], Shuanhong MA[2,3,*], Feng ZHOU[2]

[1] *Key Laboratory of Eco-functional Polymer Materials of the Ministry of Education, Key Laboratory of Polymer Materials of Gansu Province, College of Chemistry and Chemical Engineering, Northwest Normal University, Lanzhou 730070, China*

[2] *State Key Laboratory of Solid Lubrication, Lanzhou Institute of Chemical Physics, Chinese Academy of Sciences, Lanzhou 730000, China*

[3] *Shandong Laboratory of Yantai Advanced Materials and Green Manufacture, Yantai 264006, China*

Received: 28 September 2021 / Revised: 21 December 2021 / Accepted: 31 January 2022

Abstract: Osteoarthritis (OA) has been regarded as a lubrication deficiency related joint disease. Combination of both joint lubrication and drug intervention may provide a promising nonsurgical strategy for treatment of OA. Developing novel and simple approaches to fabricate superlubricating nanoparticles with drug release property is highly required. Herein, dopamine triggered one-step polymerization method was employed to fabricate polydopamine/poly(3-sulfopropyl methacrylate potassium salt) (PDA–PSPMA) conjugate coating on hollow silica (h-SiO_2) nanosphere surfaces to engineer functional nanoparticles (h-SiO_2/PDA–PSPMA). The as-prepared h-SiO_2/PDA–PSPMA exhibits excellent aqueous lubrication performance on biomaterial substrates as well as natural bovine articular cartilage based on hydration effect of negatively charged PDA–PSPMA coating and "rolling" effect of h-SiO_2 nanospheres. In vitro drug loading-release experiments demonstrate that PDA–PSPMA coating functionalized h-SiO_2 nanospheres show high drug-loading and sustained-release capability of an anti-inflammatory drug, diclofenac sodium (DS). Such h-SiO_2/PDA–PSPMA nanospheres can be potentially used as a synergistic therapy agent for OA treatment combining by simultaneous joint lubrication and drug release.

Keywords: osteoarthritis treatment; functionalized nanoparticles; injectable biolubricant; friction reduction; drug release

1 Introduction

Biological aqueous lubrication between sliding articular cartilage surfaces provides an ultralow coefficient of friction (0.001–0.03) under a wide range of conditions. Such superior lubrication remarkably decreases the wear of cartilage over decades of use [1–3]. However, a failure of articular lubrication system commonly induces increased wear of cartilage and thus osteoarthritis (OA), which gives rise to severe pain and swelling of joint [4, 5]. For early OA, it is often necessary to inject artificial joint synovial fluid as viscous supplements to improve the lubrication situation, such as hyaluronic acid (HA). However, rapid degradation of HA in vivo limits the efficiency of OA treatment and also brings the new risk of external infection caused by frequent injection [6, 7]. In addition, supplement of anti-inflammatory drugs can effectively alleviate the progression of OA. Accordingly, a synergetic therapy combining both joint lubrication and drug intervention is considered to be a promising nonsurgical strategy for treatment of OA [8–11]. Recently, hydration lubrication mechanism and the synergism between different molecular components from the synovial joints (namely hyaluronan, lubricin, and phospholipids) proposed by Klein, have been

*Corresponding authors: Qiangbing WEI, E-mail: weiqiangbing@nwnu.edu.cn; Shuanghong MA, E-mail: mashuanhong@licp.cas.cn

widely recognized to well explain the superior lubrication of articular cartilage [12–15]. Large amount of water molecules could tenaciously bind to charged biomacromolecules to form efficient hydration layer, which can serve as a fluid-like boundary film to significantly reduce friction and bear joint pressures. Inspired by hydration lubrication mechanism, researchers have been committed to develop biomimetic superlubricating materials to solve the friction and wear issues in biological systems. Meanwhile, zwitterionic polymers (e.g., phosphatidylcholine headgroups) and various polyelectrolytes were grafted onto biomaterial surfaces as biomimicking systems, which have been proved to be able to significantly reduce friction coefficient [16–21]. Furthermore, these hydrophilic polymers functionalized micro- and nano-sized particles represent another type of additives for biological aqueous lubrication. The high hydration capacity would make the particles homogeneously disperse in aqueous media and thus enhance lubrication of aqueous fluids [8, 22–25]. Additionally, the "roll" effect of nanospheres may also contribute to lubrication and anti-wear properties of aqueous fluids. For instance, ball-bearing-inspired polyampholyte-modified hydrogel microspheres were fabricated by microfluidic technique and surface grafting modification. The grafting of zwitterionic brushes enabled microspheres efficient lubrication, reduced degradation, and sustained drug release, which exhibited great potential for the treatment of OA [26].

As for oral anti-inflammatory drugs, it is difficult to reach the joint owing to lack of blood vessels in articular cartilage and small drug molecules can be quickly cleared from the joint. Therefore, encapsulating drug molecules into nanocarriers is an efficient strategy to directly deliver drugs into the joint by local injection [27, 28]. Hollow SiO_2 nanoparticles (h-SiO_2) with good biocompatibility, stable chemical properties, and the feasibility for surface functionalization, can be a representative drug nanocarrier to achieve controlled drug release [29–31]. To improve the dispersibility and endow its good hydration lubrication ability, various hydrophilic polymer brushes were grafted from SiO_2 nanoparticles surfaces by surface-initiated polymerization strategy. Liu et al. [32] grafted negatively charged poly(3-sulfopropyl methacrylate potassium salt) brushes (PSPMA) on the surface of hollow SiO_2 microspheres through surface-initiated atom transfer radical polymerization (SI-ATRP) strategy. The PSPMA-functionalized h-SiO_2 demonstrated excellent hydration lubrication performance and sustained drug release ability. Furthermore, mesoporous silica nanospheres were also grafted with PSPMA and zwitterionic poly(2-methacryloyloxyethyl phosphorylcholine) (PMPC) brushes via photopolymerization [33, 34]. The tribology and drug loading-release experiments revealed enhanced lubrication and sustained drug release behavior of the functionalized nanospheres. In addition, the in vitro and in vivo experiments suggested that the functionalized nanospheres not only protected oxidative stress-induced chondrocytes from degradation but also inhibited the development of OA. However, these methods, especially ATRP strategy, inevitably introduces toxic catalysts (e.g., copper ion) or initiators, which have a great impact on the biocompatibility and limit the biological applications of such polymer-grafted nanoparticles. Hence, developing novel and simple approaches to fabricate functional nanoparticles with simultaneous lubrication and drug-loading properties for synergetic therapy, but without utilization of complex synthesis and introduction of toxic reagents, is highly required.

Mussel-inspired polydopamine (PDA) surface chemistry has received continually increased attention since the oxidative self-polymerization of dopamine was reported [35]. In particular, PDA coating provides a versatile platform to prepare multifunctional surfaces via post-functionalization and also serves as an adhesion site to assist codeposition with targeted polymers via the non-covalent or covalent interactions [36–40]. However, the polymers used in codeposition process require to be synthesized before modification, which is not a real one-step method. Most recently, Zhang et al. [41] reported a rather simple approach to prepare PDA-polymer conjugate coatings via dopamine triggered one-step polymerization and codeposition of (methyl)acrylate monomers. In this process, dopamine molecules acted as both initiator and adhesive, which greatly simplified the reaction steps and enriched functionality of the coating. After that, dopamine triggered one-step polymerization and codeposition strategy was commonly employed

to fabricate low friction and antifouling coatings on surfaces of macroscale diverse biomaterials [42–45]. Nevertheless, few studies have investigated the surface functionalization of micro/nanoparticles with dopamine triggered polymerization of monomer, to engineer superlubricating nanoparticles as ideal drug-carrier for treatment of OA.

In our work, the novel and facile approach, dopamine triggered one-step polymerization, was employed to coat h-SiO_2 for fabricating functionalized nanospheres with dual functions of hydration lubrication and drug loading-release properties. Negatively charged 3-sulfopropyl methacrylate potassium salt (SPMA) monomer was used to prepare PDA–PSPMA conjugate coating. As demonstrated in Fig. 1, the h-SiO_2 core is designed as carrier to load and release anti-inflammatory model drugs (diclofenac sodium, DS). As for outer PDA–PSPMA coating, PDA matrix endows the coating with considerable surface adhesive ability, while the charged PSPMA segments formed from *in-situ* polymerization of monomers provide hydration lubrication effect. It is hypothesized that DS loaded h-SiO_2/PDA–PSPMA could exhibit excellent lubrication in aqueous media based on hydration effect of polymer layer and "rolling" effect of nanospheres. Concurrent with superior lubrication, it also possesses drug loading and sustained release capability. Due to facile and biocompatible fabrication strategy, this functionalized nanosphere can be used as a synergistic therapy agent for OA treatment combining by simultaneous joint lubrication and drug release.

2 Experimental

2.1 Materials

Styrene (St, AR grade), toluene, and ammonia were purchased from Shanghai Chemical Reagent Co. Tetraethyl orthosilicate (TEOS, reagent grade, 98%) and polyvinylpyrrolidone (PVP 40; average Mw, 40000) was purchased from Macklin Co., Ltd. 3-Sulfopropyl methacrylate potassium salt (SPMA, 98%) was purchased from TCI. 2,2′-bipyridine (99%) and 2,2′-azobis(2-methylpropionamidine) dihydrochloride (AIBA, 99%) were purchased from Shanghai Aladdin Reagent Co., Ltd. Dopamine hydrochloride and diclofenac sodium (98%) were purchased from Macklin Co., Ltd. The PBS buffer solution (pH = 7.4) with a phosphate concentration of 10 mM. Deionized water was used in all of the experiments. All other general reagents and solvents were of analytical grade and used without any further treatment.

2.2 Preparation of hollow SiO_2 nanoparticles

The polystyrene (PS) nanoparticles were fabricated via emulsifier-free emulsion polymerization. St (10.0 g), PVP (1.5 g), AIBA (0.26 g), and H_2O (100.0 mL) were added into a four-neck round-bottom flask (250 mL). The mixture was bubbled by nitrogen gas for 60 min and then heated to 70 °C for 24 h with mechanical agitation. After polymerization, the dispersion was dialyzed with ethanol to remove impurities to obtain the PS nanoparticles. For the preparation of PS@SiO_2

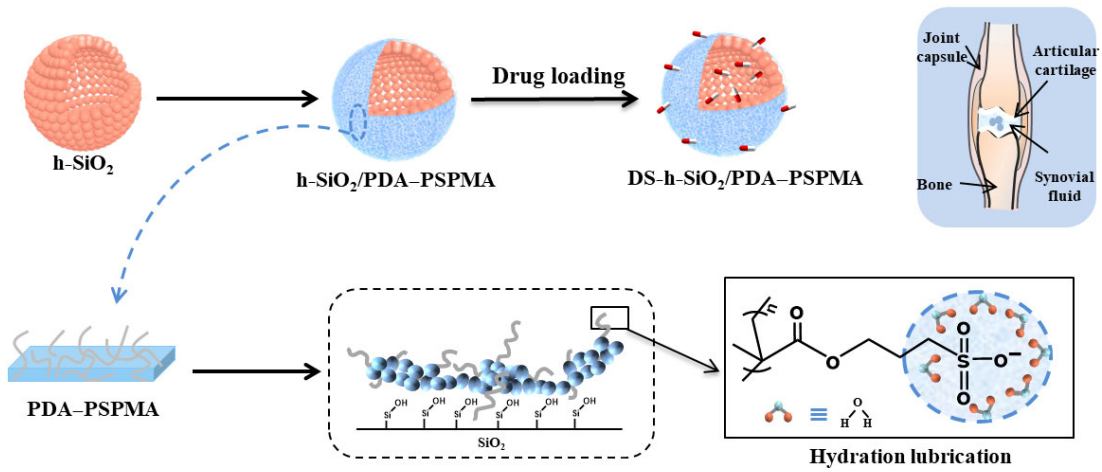

Fig. 1 Schematic illustration of the preparation of h-SiO_2/PDA–PSPMA nanospheres from dopamine-triggered one step surface functionalization.

nanoparticles, PS dispersion (3.5 g) was dissolved into 40 mL of anhydrous ethanol by ultrasonic dispersion, then TEOS (1.0 g) and ammonia (5.0 mL) were added and stirred at 50 °C for 1.5 h. The PS@SiO_2 was collected by centrifugation and washed with water and ethanol. Then the solid was dried under vacuum overnight. PS template was removed by calcining at 100 °C for 1 h, and then 600 °C for 5 h to obtain hollow SiO_2 particles (h-SiO_2).

2.3 Synthesis of h-SiO_2/PDA–PSPMA nanoparticles

100 mg of dopamine hydrochloride and SPMA monomer with desired mass were dissolved into 50 mL of Tris buffer solution (10 mM, pH = 8.5). 200 mg of h-SiO_2 nanoparticles were dispersed to the buffer solution under ultrasonication to allow the surface coating of PDA–PSPMA under stirring at ambient temperature for 24 h. After that, the brown-black solution was centrifuged and redispersed with water for three times to obtain black h-SiO_2/PDA–PSPMA nanoparticles. The resulting h-SiO_2/PDA–PSPMA sample was dried under vacuum for further characterizations.

2.4 Characterizations

The thermal properties were studied on a STA 449 C Jupiter simultaneous TG-DSC instrument (STA449F3, Germany). The element compositions were analyzed using X-ray photoelectron spectra (XPS ESCALAB 250Xi, USA). The UV absorption was recorded on an UV-vis spectrophotometer (Cary 60 UV-Vis, Agilent Technologies, USA). Field emission scanning electron microscopy (FE-SEM Quanta FEG 250, USA) and transmission electron microscopy (TEM, FEI, Tecnai, G2 TF20, USA) were employed to observe the morphology of nanoparticles. The Brunauer–Emmett–Teller (BET) measurements were performed on an ASAP 2020 (Micromeritics Instruments, USA) nitrogen adsorption instrument. The dynamic light scattering technique (DLS) was employed to measure hydrodynamic diameters and ζ-potential of nanoparticles dispersion on a particle size analyzer (Zetasizer Nano ZS, Malvern Instruments, UK) equipped with a 633 nm He–Ne laser.

2.5 Evaluation of lubrication performance

The lubrication performance of h-SiO_2 and h-SiO_2/PDA–PSPMA were evaluated by conventional pin-on-disk reciprocating tribometer (CSM Co. Ltd., Switzerland). The PDMS pins with a diameter of 6 mm and untreated silicon wafer (surface roughness: Ra ~ 0.392 nm; Rq ~0.527 nm) were employed as the friction pairs. PDMS pins were prepared from commercially available silicone elastomer kits (SYLGARD 184 silicone Elastomer, base and curing agents, Dow Corning). A polystyrene 96-well cell culture plate with a round bottom was used as a mold to prepare PDMS pins with hemispherical ends. The base and curing agent of the SYLGARD 184 elastomer kit were mixed at a mass ratio of 10:1 and transferred to the mold after removing bubbles under gentle vacuum and then incubated in an oven at 70 °C for 6 h. All the friction tests were done in a reciprocating mode and under different loads and reciprocating frequencies. h-SiO_2/PDA–PSPMA aqueous suspension with different concentrations were added between the two friction pairs as the lubricants (oscillation amplitude: 5 mm; for a duration of 3,600 sliding cycles). All samples were repeated at least three times to obtain the average value. The natural articular cartilage specimens (size: 1.5 mm × 1.0 mm) used for friction tests were derived from market from the knee joint of a cow, followed by ultrasonic treatment with 75% ethanol and PBS buffer solution for 3 times. The cartilage specimens were fixed onto the machine through commercial glue.

2.6 Preparation of calibration curves

Anti-inflammatory drug (diclofenac sodium, DS) was dissolved into PBS buffer solution (pH=7.4) and diluted to different concentrations. The UV absorbance of DS solutions was recorded, and then the calibration curves were drawn based on the different concentration of DS solutions and UV absorbance at 276 nm.

2.7 Fabrication of drug-loaded h-SiO_2/PDA–PSPMA

20 mg h-SiO_2/PDA–PSPMA and 20 mg DS were added into a beaker containing 20 mL of PBS buffer solution. The mixture was uniformly dispersed under mild ultrasonication and then stirred at 25 °C for 48 h. The obtained suspension was centrifuged at 8,000 rpm for 5 min to separate the precipitates from supernatant. The precipitates were dried under vacuum at 60 °C for 12 h and then weighed to calculate drug loading

capacity (LC). 1 mL of the supernatant was diluted and then measured by UV-vis spectrophotometer at 276 nm to calculate drug encapsulation efficiency (EE). Each sample was measured three times to ensure accuracy. The LC and EE were evaluated by the following equations, respectively. The same method was used to prepare the drug-loaded h-SiO_2.

$$\text{LC}\ (\%) = \frac{\text{Amount of loaded DS}}{\text{Amount of DS-h-SiO}_2\text{/PDA}-\text{PSPMA}} \times 100 \tag{1}$$

$$\text{EE}\ (\%) = \frac{\text{Amount of loaded DS}}{\text{Total amount of addd DS}} \times 100 \tag{2}$$

2.8 In vitro drug release

To study in vitro drug release behavior, DS-loaded h-SiO_2/PDA–PSPMA nanoparticles were dispersed in deionized water, and put into the dialysis bag (molecular weight cutoff, 8,000–10,000) at room temperature. Dialysis was carried out with 250 mL of PBS buffer solution (pH = 7.4). 3.0 mL of dialysate was taken out for absorbance test at regular intervals, and then 3.0 mL fresh PBS buffer solution was complemented. Free DS and DS-loaded h-SiO_2 were used as the references. The drug release test of DS-loaded h-SiO_2 was identical with that of DS-loaded h-SiO_2/PDA–PSPMA. As for drug release test of free DS, a certain amount of DS was dissolved in deionized water and sealed in dialysis bag (molecular weight cutoff, 8,000–10,000). Then the dialysis process was the same with that of DS-loaded h-SiO_2/PDA–PSPMA. The concentration of DS in the dialysate is calculated by UV-vis absorbance and calibration curve, and the amount of drug release can be calculated by Eq. (3):

$$\text{Drug release}\ (\%) = \frac{M_t}{M_\infty} \times 100 \tag{3}$$

where M_t is the amount of DS released from the as-prepared nanoparticles at time t, while M_∞ is the total amount of DS encapsulated by nanoparticles.

2.9 In vitro cell viability assays

The in vitro cytotoxicity of h-SiO_2/PDA–PSPMA was evaluated via standard Methyl Thiazolyl Tetrazolium (MTT) assay using C57BL/6 Mouse Mesenchymal Stem (MSC) cells. The MSC cells were seeded in a 96-well plate (100 μL/well) and cultured in a standard cell culture medium (containing 5 mL fetal bovine serum, 0.5 mL L-glutamic acid, 0.5 mL double antibody, and 45 mL basal medium) at 37 °C with 5% CO_2 for 24 h. Then h-SiO_2/PDA–PSPMA dispersions with different concentrations were added and incubated for another 48 h. Finally, the supernatants were removed while cells were washed with PBS solution. The MTT solution was added to each well and incubated at 37 °C with 5% CO_2 for 4 h. Afterwards, the supernatants were removed and 100 μL DMSO (dimethyl sulfoxide) was added to each well. The cells were further incubated for 40 min. The absorbance at 570 nm was recorded by a microplate reader to calculate the cell survival rate. The viability of cells was calculated by Eq. (4):

$$\text{Cell viability}\ (\%) = \frac{\text{OD}_{\text{h-SiO}_2\text{/PDA}-\text{PSPMA}} - \text{OD}_{\text{Blank}}}{\text{OD}_{\text{Control}} - \text{OD}_{\text{Blank}}} \times 100 \tag{4}$$

where $\text{OD}_{\text{h-SiO}_2\text{/PDA}-\text{PSPMA}}$ was obtained from h-SiO_2/PDA–PSPMA treated cells, while $\text{OD}_{\text{Control}}$ was obtained from the untreated cell and OD_{Blank} was obtained from only culture medium.

3 Results and discussion

3.1 Preparations and characterizations of h-SiO_2/PDA–PSPMA nanospheres

As shown in Fig. 1, the h-SiO_2 nanospheres were synthesized by the template method. PS nanoparticles were used as templates, which were removed by calcination after h-SiO_2 shell was coated. Then, PDA–PSPMA conjugate coating was deposited on the surface of h-SiO_2 in tris buffer solution containing dopamine molecules and SPMA monomer via dopamine triggered one-step polymerization. During the polymerization, abundant free radicals generated from the oxidative self-polymerization process of dopamine could trigger the polymerization of SPMA monomer. The *in-situ* generated PSPMA polymers would be incorporated into PDA coating [41].

The surface chemical compositions of h-SiO_2 and h-SiO_2/PDA–PSPMA were evaluated by X-ray photoelectron spectroscopy (XPS). As shown in Fig. 2(a),

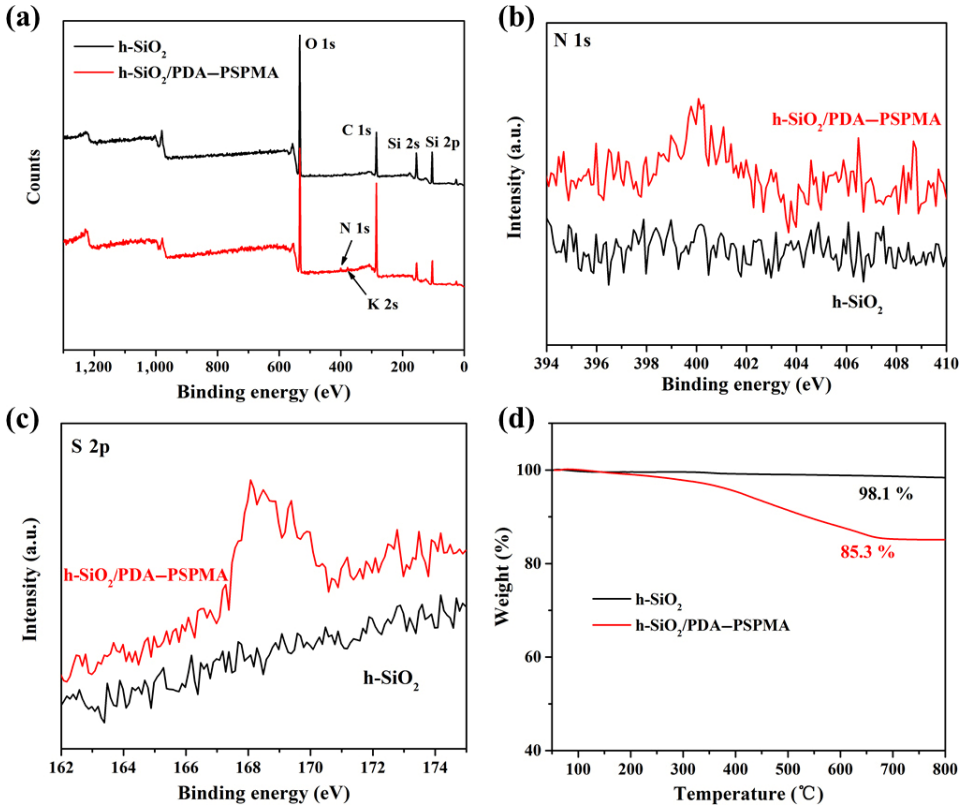

Fig. 2 (a) XPS survey spectra of h-SiO_2 and h-SiO_2/PDA—PSPMA, (b) N1s spectrum, (c) S 2p spectrum, (d) TGA curves of h-SiO_2 and h-SiO_2/PDA—PSPMA. The PDA—PSPMA coating was prepared with dopamine/SPMA mass ratio of 1:20.

the binding energies of Si 2p and Si 2s were at 103 and 153 eV, respectively, which was attributed to the silicon element in h-SiO_2 [46, 47]. After deposition of PDA–PSPMA coating, the signals of Si 2p and Si 2s were obviously decreased, indicating SiO_2 surface was covered with polymer coating. The successful deposition of PDA–PSPMA coating was further confirmed by the appearance of N 1s signal at 400 eV and S 2p signal at 168 eV, which were not found in bare h-SiO_2 [33]. To estimate the mass fraction of polymer in h-SiO_2/PDA–PSPMA hybrids, thermogravimetric analyses (TGA) of h-SiO_2 and h-SiO_2/PDA–PSPMA were conducted. As shown in Fig. 2(d), a negligible weight loss of 1.9% was observed from the curve of h-SiO_2, demonstrating the PS template was totally removed. When the PDA–PSPMA coating was deposited, the weight loss was increased to 14.7%. As a result, the mass fraction of the PDA–PSPMA coating is calculated to be 12.8%. The TGA data not only confirm the successful deposition of polymer coating on h-SiO_2 surfaces, but also provide a quantitative assessment for each component of the nanohybrids.

The morphologies of PS, h-SiO_2, and h-SiO_2/PDA–PSPMA were observed via SEM and TEM. As shown in Figs. 3(a) and 3(d), PS templates showed well-defined spherical morphology and uniform size distribution with the average diameter of ca. 290 nm. The surface of PS nanosphere was quite smooth. PS@h-SiO_2 was prepared by the sol-gel process. After the removal of PS templates by calcination, the high contrast between dark shells and light cavities suggested that PS templates were totally removed and hollow structure was formed. The surface of h-SiO_2 nanosphere became rougher and the thickness of h-SiO_2 shell was about 14 nm [32, 48, 49]. Figures 3(c) and 3(f) demonstrate the SEM and TEM images of h-SiO_2/PDA–PSPMA nanospheres, respectively. After coated with PDA–PSPMA, the morphology of h-SiO_2 was well maintained and the outer shell became less uniform and much rougher. Thickness of the shell layer was measured to be ca. 20 nm, indicating that the thickness of the PDA–PSPMA deposited layer was approximately 6 nm. TEM images also confirm that h-SiO_2 was successfully coated with PDA–PSPMA.

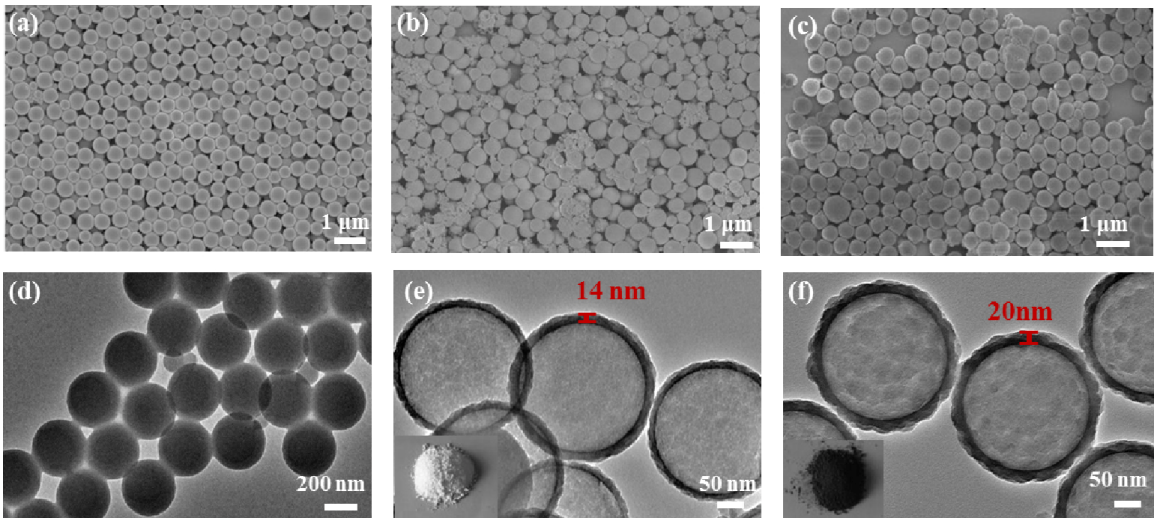

Fig. 3 SEM and TEM images of PS (a, d), h-SiO_2 (b, e), and h-SiO_2/PDA—PSPMA with dopamine/SPMA mass ratio of 1:20 (c, f). The insets of (e) and (f) are digital photos of h-SiO_2 and h-SiO_2/PDA—PSPMA powder.

To further study the porosity of h-SiO_2 and h-SiO_2/PDA–PSPMA, N_2 adsorption–desorption isotherms and corresponding pore size distribution curves of h-SiO_2 and h-SiO_2/PDA–PSPMA were measured. As shown in Fig. 4, both isotherms were in accordance with the typical IV type N_2 adsorption/desorption pattern [46], indicating that the nanoparticles have a mesoporous structure [49]. The specific surface area of h-SiO_2 was calculated to be 40.9 m^2/g according to the Brunauer–Emmett–Teller (BET) model, while the pore size was about 3.8 nm with relatively narrow distribution. Following the deposition of PDA–PSPMA coating, the specific surface area and pore size of the h-SiO_2/PDA–PSPMA were reduced to about 29.2 m^2/g, and about 3.1 nm, respectively. As for h-SiO_2/PDA–PSPMA, the decrease of specific surface area and pore size was attributed to the coverage of PDA–PSPMA polymer layer on h-SiO_2 surface. The relatively large specific surface area and cavity structure of h-SiO_2/PDA–PSPMA nanospheres provided enough space for drug loading, and the pores on the surface provide channels for drug loading and release [46, 48].

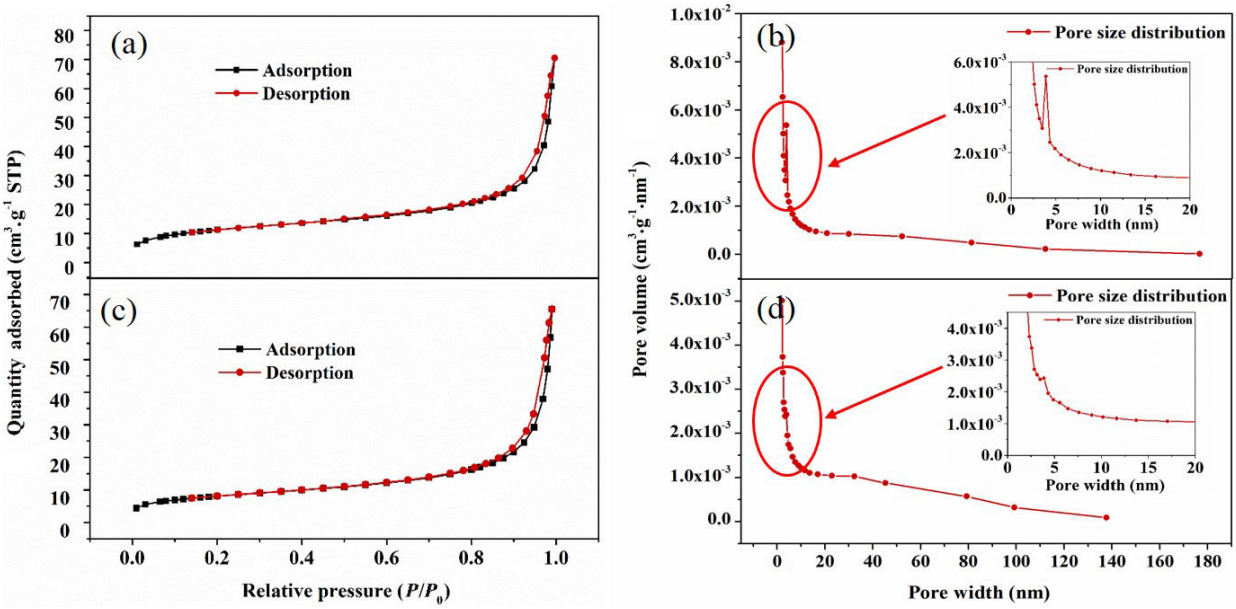

Fig. 4 N_2 adsorption–desorption isotherms and pore size distribution curves of h-SiO_2 (a, b) and h-SiO_2/PDA–PSPMA (c, d).

The hydrodynamic diameter and ζ-potential of nanospheres in aqueous media were evaluated using dynamic light scattering (DLS). Figure 5 shows the DLS intensity distribution of h-SiO_2 and h-SiO_2/PDA–PSPMA at 25 °C in aqueous solution. The corresponding average diameters and ζ-potentials were summarized in Table 1. The hydrodynamic diameter of h-SiO_2 was about 373.2 nm, which was a little bit larger than the average diameter of h-SiO_2 in dry state (317.1 nm). This is due to adsorbed hydration layer on h-SiO_2 surface. The hydrodynamic diameter of h-SiO_2/PDA–PSPMA was around 471.8 nm, which was much larger than that of h-SiO_2. Furthermore, as shown in Table 1, after coated with PDA–PSPMA, the ζ-potential of the nanospheres changed from nearly neutral to negative (ca. –7.8 mV). These results further verified that negatively charged PDA–PSPMA coating was successfully deposited on h-SiO_2 surfaces. It was worth noting that the hydrodynamic diameter of h-SiO_2/PDA–PSPMA was much larger than that in in dry state (328.2 nm) tested by TEM. This is due to high hydration capacity of negatively charged PSPMA. PDA–PSPMA conjugate coating could swell and form a hydration layer by combining large amount of water molecules [50]. Therefore, DLS analysis demonstrated that the PDA–PSPMA coated h-SiO_2 dispersions with high hydration have a great potential for aqueous lubrication [51].

3.2 Evaluation of lubrication performance

The lubrication performance of h-SiO_2/PDA–PSPMA aqueous dispersion was evaluated on a ball-on-disk reciprocating tribometer using silicon wafers and PDMS soft balls as friction pairs. The coefficients of friction (COF) of pure water, bare h-SiO_2 as well as PDA coated h-SiO_2 (h-SiO_2/PDA) were also presented as comparisons.

Figure 6(a) shows the COF vs time plots of different samples under the load of 0.5 N and with the reciprocating frequency of 1 Hz. The high/non-stable COF of water can be attributed to its low viscosity and large elastic deformation along with rising wear of PDMS pair. Compared with pure water, bare h-SiO_2 dispersion (2 mg/mL) exhibited obvious friction-reduction property with average COF of ~0.3, possibly due to "rolling" effect of spherical nanoparticles. However, the COF becomes non-stable and increased obviously after 2,200 s, the reason for this may be that the hollow nanoparticles were broken under dynamic shearing process. In contrast, h-SiO_2/PDA–PSPMA dispersion displayed ultralow COF after 200 s of "running in" process and could keep in constant even

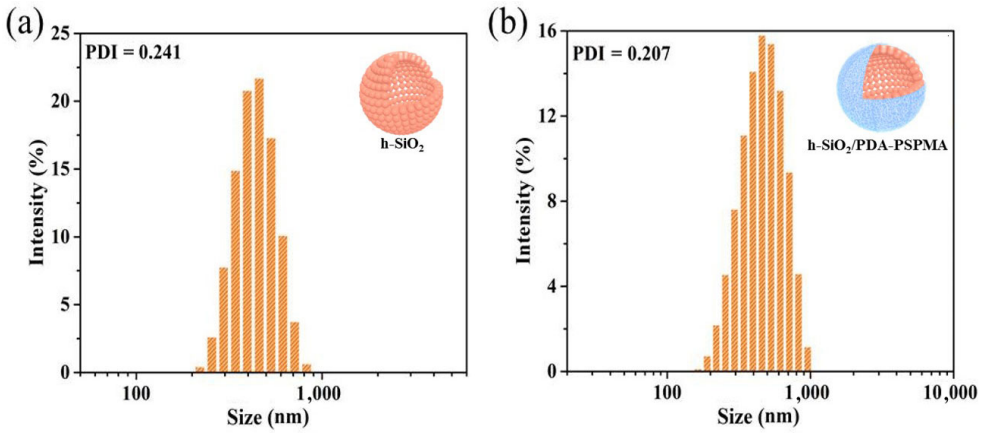

Fig. 5 Hydrodynamic diameter distribution of h-SiO_2 (a) and h-SiO_2/PDA—PSPMA (b) in aqueous media at 25 °C.

Table 1 Hydrodynamic diameter and ζ-potential analysis of h-SiO_2 and h-SiO_2/PDA—PSPMA with dopamine/SPMA mass ratio of 1:20.

Sample	ζ (mV)	D_{dry} (nm)	D_h (nm)
h-SiO_2	0.04 ± 0.09	317.1 ± 8.7	373.2 ± 2.0
h-SiO_2/PDA–PSPMA	–7.8 ± 0.8	328.2 ± 3.8	471.8 ± 3.7

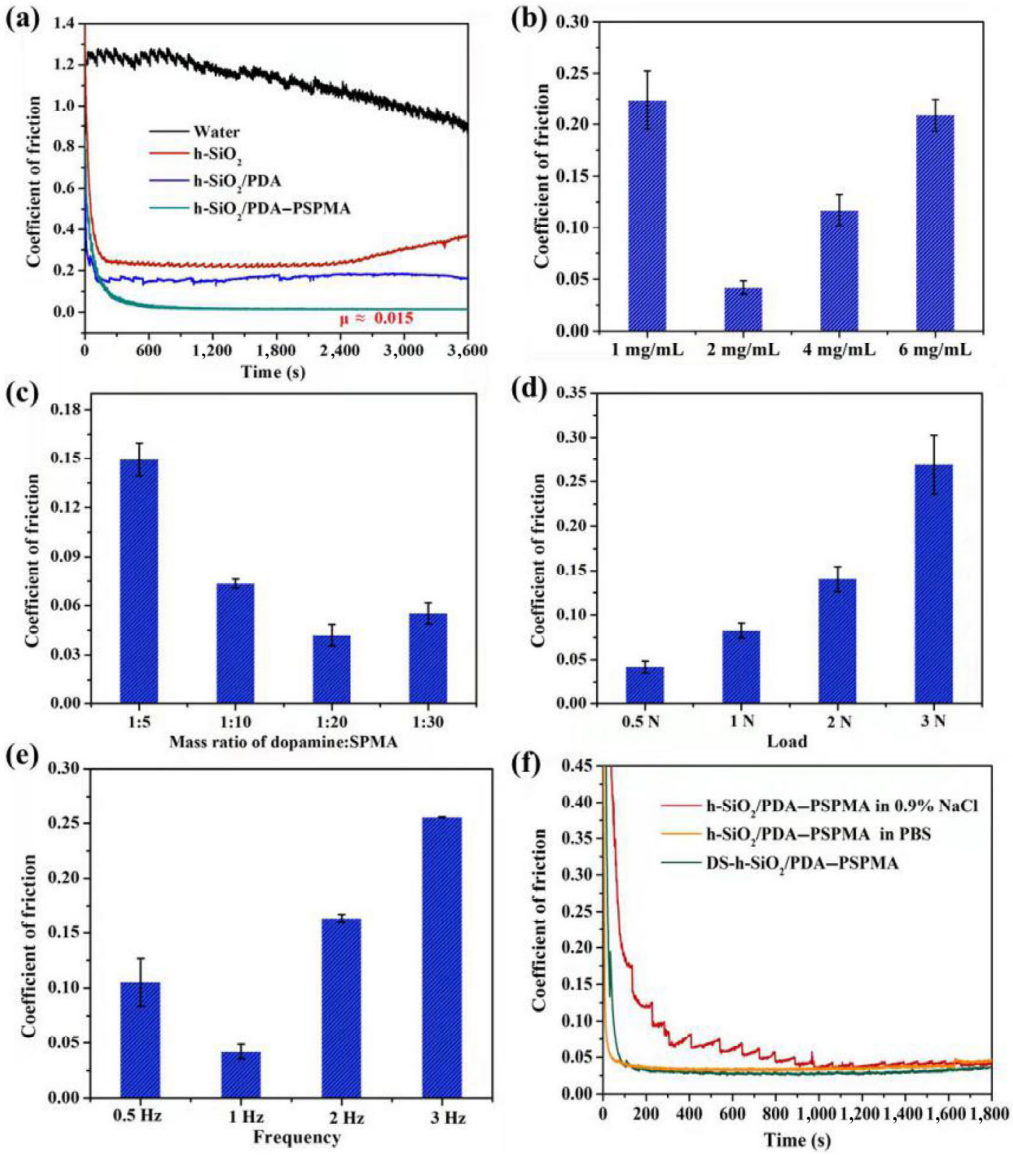

Fig. 6 Tribological properties of different samples. (a) COFs vs time curves of pure water, h-SiO_2, h-SiO_2/PDA, and h-SiO_2/PDA–PSPMA in aqueous dispersion; (b) mean COF of h-SiO_2/PDA–PSPMA (dopamine/SPMA = 1:20) dispersion with different concentrations; (c) mean COFs of h-SiO_2/PDA–PSPMA with different mass ratios of dopamine/SPMA; (d) mean COFs of h-SiO_2/PDA–PSPMA under different contact loads (the corresponding contact pressures are 0.42, 0.53, 0.67, and 0.77 MPa, respectively); (e) mean COFs of h-SiO_2/PDA–PSPMA with different reciprocating frequencies; (f) COFs vs time curves of DS-h-SiO_2/PDA–PSPMA and h-SiO_2/PDA–PSPMA in different physiological solutions.

after 3,600 sliding cycles. The COF of h-SiO_2/PDA–PSPMA was as low as 0.015, decreasing by 95% compared with that of bare h-SiO_2. Further, the COF of h-SiO_2/PDA–PSPMA was also one order of magnitude lower than that of h-SiO_2/PDA dispersion (COF~0.16), suggesting that *in-situ* formed PSPMA segments have essential contribution for the friction-reduction of h-SiO_2 dispersion via hydration mechanism. The lubrication performance of h-SiO_2/PDA–PSPMA dispersion with different concentrations (reciprocating frequency: 1 Hz; loading force: 0.5 N; and mass ratio of dopamine/SPMA = 1:20) was investigated and shown in Fig. 6(b). With increasing the concentration of h-SiO_2/PDA–PSPMA dispersion from 1 to 2 mg/mL, the mean COF decreased from 0.22 to 0.04. While continually increasing the concentration of dispersion (from 2 to 4 and 6 mg/mL), the mean COF showed an increasing trend, from 0.04 to 0.12 and then 0.21.

These results illustrated that high concentrations of h-SiO_2/PDA–PSPMA would lead to relatively poor lubricating properties. This is because high concentration dispersion may result in agglomeration of nanoparticle and thus poor lubrication.

According to previous reports, acrylate monomers in the system can inhibit the formation of PDA nanoaggregates and then decrease adhesion and deposition of PDA species on solid surface [52]. Therefore, the effect of mass ratios of dopamine/SPMA (content of SPMA monomer) on the tribological properties of h-SiO_2/PDA–PSPMA were investigated (loading force: 0.5 N; reciprocating frequency: 1 Hz; and concentration: 2 mg/mL). As shown in Fig. 6(c), the average COF decreased from 0.15 to 0.07 and then 0.04 with increasing the content of SPMA monomer (the corresponding dopamine/SPMA mass ratios were 1:5, 1:10, and 1:20, respectively). h-SiO_2/PDA–PSPMA prepared with dopamine/SPMA mass ratio of 1:20 exhibited best lubrication. When dopamine/SPMA mass ratio is 1:30, the COF was slightly increased to 0.05. This phenomenon is resulted from the fact that high concentration of SPMA can inhibit the formation of PDA nanoaggregates and then influence the deposition of PDA on h-SiO_2 surface. Afterward, the lubrication performance of h-SiO_2/PDA–PSPMA under different loading force and at different reciprocating frequency were evaluated. With increasing the normal loads from 0.5 to 3 N, the COF gradually increased (Fig. 6(d)), which was attributed to the deformation of soft PDMS as well as partially damage of PDA–PSPMA hydration layer surrounding h-SiO_2 nanospheres. In Fig. 6(e), the COF presented a decreasing trend with increasing the reciprocating frequency from 0.5 to 1 Hz, while it began to increase when reciprocating frequency was larger than 1 Hz. As h-SiO_2/PDA–PSPMA was intended to reduce friction and load drugs for sustained release in biological media. It is necessary to study the lubrication performance of drug-loaded h-SiO_2/PDA–PSPMA (DS-h-SiO_2/PDA–PSPMA) and h-SiO_2/PDA–PSPMA in saline solution (0.9% NaCl) and PBS buffer (pH = 7.4). As shown in Fig. 6(f), DS-h-SiO_2/PDA–PSPMA also exhibited excellent lubrication in water with average COF of 0.03, indicating that loading of DS drug doesn't influence the superior lubrication of h-SiO_2/PDA–PSPMA. The average COFs of h-SiO_2/PDA–PSPMA were approximately 0.06 and 0.10 in PBS buffer and saline solution, respectively. Comparing with the COF in pure water, h-SiO_2/PDA–PSPMA could maintain the superior lubrication in PBS buffer, whereas the lubrication capability was slightly weakened in saline solution. This slight increase of COF was possibly attributed to the partially dehydration of PSPMA chains in the coating arising from electrostatic screening effect of electrolytes. But h-SiO_2/PDA–PSPMA still showed much better lubrication than h-SiO_2/PDA and h-SiO_2 even though the slight increase of COF in saline.

To examine the feasibility of h-SiO_2/PDA–PSPMA dispersion on different substrates, the tribological tests were also performed on titanium alloy (Ti_6Al_4V), stainless steel (316L), glass, and even articular cartilage. As shown in Fig. 7(a), it was clear that h-SiO_2/PDA–PSPMA water dispersion presented very good lubrication properties on commonly used biomaterials surfaces. The slight increase in COFs on Ti_6Al_4V and 316L may be caused by relatively large roughness of the substrates. Particularly, h-SiO_2/PDA–PSPMA showed very efficient lubrication on articular cartilage with low COF of ca. 0.022, demonstrating its promising potential as injectable lubricants for restoring the lubrication of joints with loss of lubrication function. Figure 6(b) showed the comparison of lubrication capability of as-prepared h-SiO_2/PDA–PSPMA with commercially available biolubricants, hyaluronic acid (HA), and bovine serum albumin (BSA). The articular cartilages were used as friction pairs for both two sides. It could be seen that h-SiO_2/PDA–PSPMA exhibited much better lubrication than BSA aqueous solution. Furthermore, the friction curve of h-SiO_2/PDA–PSPMA without "running in" process showed similar trend with that of HA, suggesting the efficient lubrication capability of these two lubricants. However, the average COF of h-SiO_2/PDA–PSPMA (0.021) was lower than that of HA (0.024) on articular cartilage surfaces, indicating that h-SiO_2/PDA–PSPMA was more efficient than commercial HA for lubrication of degraded cartilage.

Based on the friction results of h-SiO_2/PDA–PSPMA, a plausible lubrication mechanism of h-SiO_2/PDA–PSPMA nanoparticles was proposed and given in Fig. 8. The superior lubrication of h-SiO_2/PDA–PSPMA

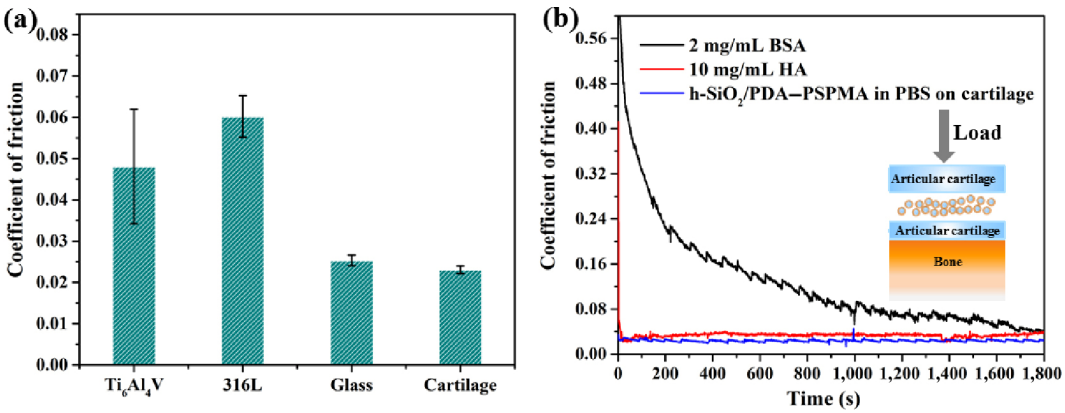

Fig. 7 (a) COFs of h-SiO_2/PDA–PSPMA on the surface of different substrates and articular cartilage; (b) COF curves of h-SiO_2/PDA–PSPMA and commercially available HA and BSA biolubricants (load: 0.5 N; reciprocating frequency: 1 Hz).

was achieved by the combination of hydration lubrication and rolling lubrication effect [53]. The negatively charged PDA–PSPMA coating on surface of h-SiO_2 nanoparticles could form efficient hydration layer for achieving good hydration lubrication [54]. Meanwhile, hydration layer formed by charged SO_3^- groups and water molecules could bear normal pressure. At the same time, the bounded water molecules exchange with free water molecules fast to give a fluid-like interface. Such fluid-like interface surrounding the nanoparticles results in ultralow COF under shearing condition. Additionally, the hydration layer could prevent h-SiO_2/PDA–PSPMA nanoparticles from aggregation. Thus, it can be speculated that the free rolling of h-SiO_2/PDA–PSPMA nanoparticles may employ a rolling mechanism to reduce friction between sliding surfaces. In this case, the soft and fluid-like PDA–PSPMA hydration layer and the hard h-SiO_2 nanoparticles play a synergistic effect and co-contribute to the superior lubrication of h-SiO_2/PDA–PSPMA water dispersion.

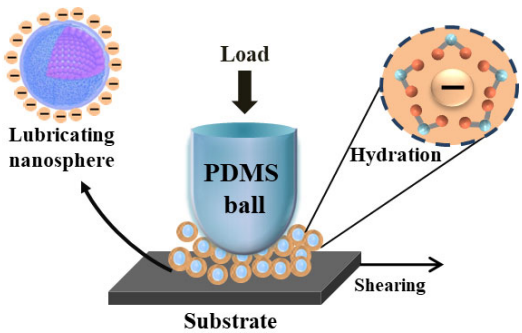

Fig.8 Schematic diagram of lubrication mechanism of h-SiO_2/PDA–PSPMA.

3.3 In vitro drug loading and release

As h-SiO_2/PDA–PSPMA nanospheres could achieve a ultralow COF in aqueous media as well as biological fluids, which is expected to be a promising biological lubricant for treatment of OA. In addition, the hollow structure and rich pores on the surface make h-SiO_2/PDA–PSPMA nanospheres as an ideal drug carrier for drug loading and release. The h-SiO_2/PDA–PSPMA nanospheres can realize the dual function of lubrication and drug loading. Herein, DS, an anti-inflammatory and analgesic drug for OA treatment, was used as a model drug to evaluate sustained release property of h-SiO_2/PDA–PSPMA. The calibration curve and chemical structure of DS were presented in Fig. 9(a). The DS-loaded h-SiO_2 and DS-loaded h-SiO_2/PDA–PSPMA were obtained by centrifugation to separate solid nanospheres from supernatant after stirring for 48 h. The calculated LC and EE of DS were 32.4% and 58.1%, respectively, which demonstrates that h-SiO_2/PDA–PSPMA has a good drug loading capacity. Figure 9(b) shows the DS release profiles of free DS, h-SiO_2, and h-SiO_2/PDA–PSPMA. It can be found that free DS without any carrier was almost 100% released within 27 h. In contrast, within 27 h, the cumulative release for h-SiO_2 and h-SiO_2/PDA–PSPMA were 62% and 46%, respectively. It was clear that the drug release profile of h-SiO_2/PDA–PSPMA was always below that of h-SiO_2. The cumulative release of DS within 72 h could reach 74.9% for h-SiO_2, while it was only 59.9% for h-SiO_2/PDA–PSPMA. Compared with h-SiO_2, h-SiO_2/PDA–PSPMA displayed obvious sustained release effect, owing to the coverage of PDA–PSPMA

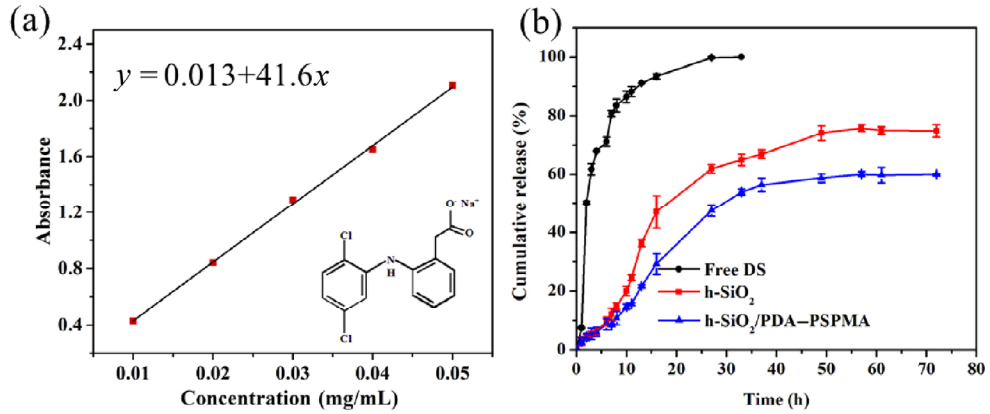

Fig. 9 (a) Calibration curve of DS based on the UV absorption (the inset is chemical structure of DS) and (b) DS release profiles from free DS, h-SiO_2, and h-SiO_2/PDA–PSPMA within 72 h in PBS buffer solutions (pH = 7.4) at room temperature.

coating on h-SiO_2 nanospheres. Because of the collapse of PDA–PSPMA conjugate coating in dry state, the loaded DS was completely encapsulated in the interior cavity of h-SiO_2/PDA–PSPMA. In aqueous media, the hydration and swelling of PDA–PSPMA conjugate coating could allow for the diffusion and release of DS drug to the outside through the channels on h-SiO_2 surfaces [55]. These results demonstrated that h-SiO_2/PDA–PSPMA possessed good drug loading capacity and sustained release performance.

3.4 In vitro cytotoxicity

Nontoxicity or low toxicity is a critical parameter for biomedical applications of h-SiO_2/PDA–PSPMA nanospheres. Therefore, in vitro cytotoxicity was investigated by MTT assay. MSC cells were incubated with different concentration of h-SiO_2/PDA–PSPMA nanospheres for 48 h. As shown in Fig. 10, compared with control group, the cell viability of experimental groups was basically not significantly reduced. The cell viability remained around 85% in the range of 0.78–200 μg/mL, indicating that the good biocompatibility of h-SiO_2/PDA–PSPMA for MSC cells. These results demonstrated that the biocompatible h-SiO_2/PDA–PSPMA nanospheres with ultralow-friction performance and sustained drug release property would realize simultaneous cartilage lubrication and OA treatment.

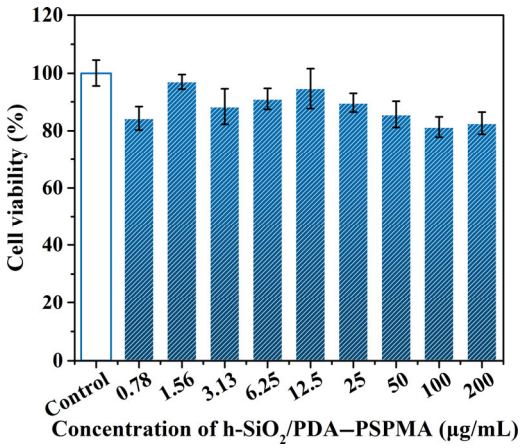

Fig. 10 Cell viability incubated for 48 h with different concentrations of h-SiO_2/PDA–PSPMA.

4 Conclusions

In this work, the dopamine-triggered one-step surface functionalization method was introduced to coat h-SiO_2 with PDA–PSPMA conjugate coating for developing dual functional nanospheres (h-SiO_2/PDA–PSPMA) with simultaneous aqueous lubrication and drug release properties. A series of characterizations were employed to confirm the successful fabrication of h-SiO_2/PDA–PSPMA. The lubrication tests results reveal that obtained h-SiO_2/PDA–PSPMA nanospheres exhibit superior aqueous lubrication performance on biomaterial substrates as well as natural bovine articular cartilage, mainly attributing to hydration mechanism of negatively charged PDA–PSPMA coating and free "rolling effect" of spherical h-SiO_2 nanoparticles. Moreover, in vitro drug release demonstrates that h-SiO_2/PDA–PSPMA possesses a good drug loading and sustained release abilities of an anti-inflammatory drug (e.g., DS). Due to facile fabrication strategy, efficient lubrication, drug loading and release behavior, as well as good biocompatibility,

h-SiO_2/PDA–PSPMA nanospheres can be potentially used as a synergistic therapy agent for arthritis treatment combining by simultaneous joint lubrication and drug sustained release.

Acknowledgements

This work was financially supported by National Natural Science Foundation of China (52065061, 22032006), Outstanding Youth Fund of Gansu Province (21JR7RA158, 21JR7RA095), Innovation Fund for Universities of Gansu Province (2021A-015), and Youth Innovation Promotion Association CAS (2019411).

References

[1] Stachowiak G, Batchelor A, Griffiths L. Friction and wear changes in synovial joints. *Wear* **171**(1–2): 135–142 (1994)

[2] Klein J. Molecular mechanisms of synovial joint lubrication. *Proc Inst Mech Eng Part J J Eng Tribol* **220**(8): 691–710 (2006)

[3] Jahn S, Seror J, Klein J. Lubrication of articular cartilage. *Annu Rev Biomed Eng* **18**(1): 235–258 (2016)

[4] Ji X, Zhang H. Current strategies for the treatment of early stage osteoarthritis. *Front Mech Eng* **5**: 57 (2019)

[5] Lin W, Klein J, Recent progress in cartilage lubrication. *Adv Mater* **33**(18): 2005513 (2021)

[6] Jean Y, Wen Z, Chang Y, Lee H, Hsieh S, Wu C, Yeh C, Wong C. Hyaluronic acid attenuates osteoarthritis development in the anterior cruciate ligament-transected knee: Association with excitatory amino acid release in the joint dialysate. *J Orthop Soc* **24**(5): 1052–1061 (2006)

[7] Vincent H K. Hyaluronic acid (HA) viscosupplementation on synovial fluid inflammation in knee osteoarthritis: A pilot study. *Open Orthop J* **7**: 378–384 (2013)

[8] Liu G, Liu Z, Li N, Wang X, Zhou F, Liu W. Hairy polyelectrolyte brushes-grafted thermosensitive microgels as artificial synovial fluid for simultaneous biomimetic lubrication and arthritis treatment. *ACS Appl Mater Inter* **6**(22): 20452–20463 (2014)

[9] Sun Y, Zhang H, Wang Y, Wang Y. Charged polymer brushes-coated mesoporous silica nanoparticles for osteoarthritis therapy: A combination between hydration lubrication and drug delivery. *J Control Release* **259**: e45–e46 (2017)

[10] Zhao W, Wang H, Wang H, Han Y, Zheng Z, Liu X, Feng B, Zhang H. Light-responsive dual-functional biodegradable mesoporous silica nanoparticles with drug delivery and lubrication enhancement for the treatment of osteoarthritis. *Nanoscale* **13**(13): 6394–6399 (2021)

[11] Zhang K, Yang J L, Sun Y L, Wang Y, Liang J, Luo J, Cui W G, Deng L F, Xu X Y, Wang B, Zhang H Y. Gelatin-based composite hydrogels with biomimetic lubrication and sustained drug release. *Friction* **10**(2): 232–246 (2022)

[12] Klein J. Hydration lubrication. *Friction* **1**(1): 1–23 (2013)

[13] Jahn S, Klein J. Hydration lubrication: The macromolecular domain. *Macromolecules* **48**(15): 5059–5075 (2015)

[14] Coles J, Chang D. Molecular mechanisms of aqueous boundary lubrication by mucinous glycoproteins. *Curr Opin Colloid Interface Sci* **15**(6): 406–416 (2010)

[15] Dėdinaitė A. Biomimetic lubrication. *Soft Matter* **8**(2): 273–284 (2012)

[16] Adibnia V, Mirbagheri M, Faivre J, Robert J, Lee J, Matyjaszewski K, Lee D W, Banquy X. Bioinspired polymers for lubrication and wear resistance. *Prog Polym Sci* **110**: 101298 (2020)

[17] Zheng Y, Yang J, Liang J, Xu X, Cui W, Deng L, Zhang H. Bioinspired hyaluronic acid/phosphorylcholine polymer with enhanced lubrication and anti-inflammation. *Biomacromolecules* **20**(11): 4135–4142 (2019)

[18] Wei Q, Cai M, Zhou F, Liu W. Dramatically tuning friction using responsive polyelectrolyte brushes. *Macromolecules* **46**(23): 9368–9379 (2013)

[19] Chen M, Briscoe W H, Armes S P, Klein J. Lubrication at physiological pressures by polyzwitterionic brushes. *Science* **323**(5922): 1698–1701 (2009)

[20] Wei Q, Pei X, Hao J, Cai M, Zhou F, Liu W. Surface modification of diamond-like carbon film with polymer brushes using a bio-inspired catechol anchor for excellent

biological lubrication. *Adv Mater Interfaces* **1**(5): 1400035 (2014)

[21] Gao L Y, Zhao X D, Ma S H, Ma Z F, Cai M R, Liang Y M, Zhou F. Constructing a biomimetic robust bi-layered hydrophilic lubrication coating on surface of silicone elastomer. *Friction* **10**(7): 1032–1046 (2022)

[22] Li Z, Ma S, Zhang G, Wang D, Zhou F. Soft/hard-coupled amphiphilic polymer nanospheres for water lubrication. *ACS Appl Mater Interface* **10**(10): 9178–9187 (2018)

[23] Lin W, Kampf N, Klein J. Designer nanoparticles as robust superlubrication vectors. *ACS Nano* **14**(6): 7008–7017 (2020)

[24] Zhao W, Wang H, Han Y, Wang H, Sun Y, Zhang H. Dopamine/phosphorylcholine copolymer as an efficient joint lubricant and ros scavenger for the treatment of osteoarthritis. *ACS Appl Mater Interface* **12**(46): 51236–51248 (2020)

[25] Wang C B, Bai X Q, Dong C L, Guo Z W, Yuan C Q, Neville A. Designing soft/hard double network hydrogel microsphere/UHMWPE composites to promote water lubrication performance. *Friction* **9**(3): 551–568 (2021)

[26] Yang J, Han Y, Lin J, Zhu Y, Wang F, Deng L, Zhang H, Xu X, Cui W. Ball-bearing-inspired polyampholyte-modified microspheres as bio-lubricants attenuate osteoarthritis. *Small* **16**(44): 2004519 (2020)

[27] Rahimi M, Charmi G, Matyjaszewski K, Banquy X, Pietrasik J. Recent developments in natural and synthetic polymeric drug delivery systems used for the treatment of osteoarthritis. *Acta Biomater* **123**: 31–50 (2021)

[28] Han Y, Liu S, Sun Y, Gu Y, Zhang H. Bioinspired surface functionalization of titanium for enhanced lubrication and sustained drug release. *Langmuir* **35**(20): 6735–6741 (2019)

[29] Deng C, Zhang Q, Fu C, Zhou F, Yang W, Yi D, Wang X, Tang Y, Caruso F, Wang Y. Template-free synthesis of chemically asymmetric silica nanotubes for selective cargo loading and sustained drug release. *Chem Mater* **31**(11): 4291–4298 (2019)

[30] Manzano M, Vallet-Regí M. Mesoporous silica nanoparticles for drug delivery. *Adv Funct Mater* **30**(2): 1902634 (2019)

[31] Tan X, Sun Y, Sun T, Zhang H. Mechanised lubricating silica nanoparticles for on-command cargo release on simulated surfaces of joint cavities. *Chem Commun* **55**(18): 2593–2596 (2019)

[32] Liu G, Cai M, Zhou F, Liu W. Charged polymer brushes-grafted hollow silica nanoparticles as a novel promising material for simultaneous joint lubrication and treatment. *J Phys Chem B* **118**(18): 4920–4931 (2014)

[33] Yan Y, Sun T, Zhang H, Ji X, Sun Y, Zhao X, Deng L, Qi J, Cui W, Santos H A, Zhang H. Euryale ferox seed-inspired superlubricated nanoparticles for treatment of osteoarthritis. *Adv Funct Mater* **29**(4): 1807559 (2019)

[34] Chen H, Sun T, Yan Y, Ji X, Sun Y, Zhao X, Qi J, Cui W, Deng L, Zhang H. Cartilage matrix-inspired biomimetic superlubricated nanospheres for treatment of osteoarthritis. *Biomaterials* **242**:119931 (2020)

[35] Lee H, Dellatore S M, Miller W M, Messersmith P B. Mussel-inspired surface chemistry for multifunctional coatings. *Science* **318**(5849): 426–430 (2007)

[36] Sheng W, Li B, Wang X, Dai B, Yu B, Jia X, Zhou F. Brushing up from "anywhere" under sunlight: A universal surface-initiated polymerization from polydopamine-coated surfaces. *Chem Sci* **6**(3): 2068–2073 (2015)

[37] Ryu J H, Messersmith P B, Lee H. Polydopamine surface chemistry: A decade of discovery. *ACS Appl Mater Interface* **10**(9): 7523–7540 (2018)

[38] Behboodi-Sadabad F, Zhang H, Trouillet V, Welle A, Plumeré N, Levkin P A. UV-triggered polymerization, deposition, and patterning of plant phenolic compounds. *Adv Funct Mater* **27**(22): 1700127 (2017)

[39] He Y, Xu L, Feng X, Zhao Y, Chen L. Dopamine-induced nonionic polymer coatings for significantly enhancing separation and antifouling properties of polymer membranes: Codeposition versus sequential deposition. *J Membrane Sci* **529**(1): 421–431 (2017)

[40] Qiu W Z, Yang H C, Xu Z K. Dopamine-assisted co-deposition: An emerging and promising strategy for surface modification. *Adv Colloid Interface* **256**: 111–125 (2018)

[41] Zhang C, Ma M Q, Chen T T, Zhang H, Hu D F, Wu B H, Ji J, Xu Z K. Dopamine-triggered one-step polymerization and codeposition of acrylate monomers for functional coatings. *ACS Appl Mater Interface* **9**(39): 34356–34366 (2017)

[42] Wei Q, Liu X, Yue Q, Ma S, Zhou F. Mussel-inspired one-step fabrication of ultralow-friction coatings on diverse biomaterial surfaces. *Langmuir* **35**(24): 8068–8075 (2019)

[43] Ma M Q, Zhang C, Chen T T, Yang J, Wang J J, Ji J, Xu Z K. Bioinspired polydopamine/polyzwitterion coatings for underwater anti-oil and -freezing surfaces. *Langmuir* **35**(5): 1895–1901 (2019)

[44] Wang J, Tian J, Gao S, Shi W, Cui F. Dopamine triggered one step polymerization and codeposition of reactive surfactant on pes membrane surface for antifouling modification. *Sep Purif Technol* **249**: 117148 (2020)

[45] Zhu Z, Gao Q, Long Z, Huo Q, Ge Y, Vianney N, Daliko N A, Meng Y, Qu J, Chen H, et al. Polydopamine/poly(sulfobetaine methacrylate) co-deposition coatings triggered by $CuSO_4/H_2O_2$ on implants for improved surface hemocompatibility and antibacterial activity. *Bioact Mater* **6**(8): 2546–2556 (2021)

[46] Liu Q, Zhou Y, Li M, Zhao L, Ren J, Li D, Tan Z, Wang K, Li H, Hussain M, et al. Polyethylenimine hybrid thin-shell hollow mesoporous silica nanoparticles as vaccine self-adjuvants for cancer immunotherapy. *ACS Appl Mater Interface* **11**(51): 47798–47809 (2019)

[47] Zhang Y, Zhao Y, Cao S, Yin Z, Cheng L, Wu L. Design and synthesis of hierarchical SiO_2@C/TiO_2 hollow spheres for high-performance supercapacitors. *ACS Appl Mater Interface* **9**(35): 29982–29991 (2017)

[48] Qu Z, Yao L, Li J, He J, Mi J, Ma S, Tang S, Feng L. Bifunctional template-induced VO_2@SiO_2 dual-shelled hollow nanosphere-based coatings for smart windows. *ACS Appl Mater Interface* **11**(17): 15960–15968 (2019)

[49] Tiansong D, Frank M. Synthesis of monodisperse polystyrene@vinyl-SiO_2 core–shell particles and hollow SiO_2 spheres. *Chem Mater* **24**(3): 536–542 (2012)

[50] Li Z, Ma S, Zhang G, Wang D, Zhou F. Soft/hard-coupled amphiphilic polymer nanospheres for water lubrication. *ACS Appl Mater Interface* **10**(10): 9178–9187 (2018)

[51] Liu G, Wang D, Zhou F, Liu W. Electrostatic self-assembly of Au nanoparticles onto thermosensitive magnetic core–shell microgels for thermally tunable and magnetically recyclable catalysis. *Small* **11**(23): 2807–2816 (2015)

[52] Mei Y, Yu K, Lo J C Y, Takeuch L E, Hadjesfandiari N, Yazdani-Ahmadabadi H, Brooks D E, Lange D, Kizhakkedathu J N. Polymer–nanoparticle interaction as a design principle in the development of a durable ultrathin universal binary antibiofilm coating with long-term activity. *ACS Nano* **12**(12): 11881–11891 (2018)

[53] Tevet O, Von-Huth P, Popovitz-Biro R, Rosentsveig R, Wagner H D, Tenne R. Friction mechanism of individual multilayered nanoparticles. *Proc Natl Acad Sci U S A* **108**(50): 19901–19906 (2011)

[54] Ma L, Gaisinskaya-Kipnis A, Kampf N, Klein J. Origins of hydration lubrication. *Nat Commun* **6**: 6060 (2015)

[55] Tang F, Li L, Chen D. Mesoporous silica nanoparticles: Synthesis, biocompatibility and drug delivery. *Adv Mater* **24**(12): 1504–1534 (2012)

Qiangbing WEI. He received his Ph.D. degree from Lanzhou Institute of Chemical Physics, Chinese Academy of Sciences in 2014. Then, he joined the School of Chemistry and Chemical Engineering, Northwest Normal University (NWNU) and currently is an associate professor. He did postdoctoral research in Matyjaszewski Polymer Group at Carnegie Mellon University from 2018 to 2020. His research interests include controlled radical polymerization, polymer-based materials for biomimetic lubrication and antibacterial applications, and polymer-liquid metal soft nanocomposites for flexible and wearable sensors.

Shuanhong MA. He received his Ph.D. degree from Lanzhou Institute of Chemical Physics, Chinese Academy of Sciences in 2016. Then, he joined the State Key Laboratory of Solid Lubrication and currently is an associate professor. He published more than 45 papers as the first or corresponding author in *Nature Communications*, *Matter*, *Advanced Materials*, *Angewandte Chemie International Edition*, *Advanced Functional Materials*, *Chemistry of Materials*, *Advanced Science*, *Small*, *Friction*, et al. His papers have been cited nearly 2,000 times. He has applied for 30 patents and 16 of them have been authorized. His research interests include surface lubrication modification, high performance water lubricating materials, soft matter mechanics, and the mechanism between interface contact and lubrication.